

# Stable higher-order vortex quantum droplets in an annular potential

Liangwei Dong\*

*Department of Physics, Zhejiang University of Science and Technology, Hangzhou, China, 310023*

Mingjing Fan

*Department of Physics, Shaanxi University of Science & Technology, Xi'an, China, 710021*

Boris A. Malomed

*Instituto de Alta Investigacion, Universidad de Tarapaca, Casilla 7D, Arica, Chile\*\**

arXiv:2401.07011v1 [cond-mat.quant-gas] 13 Jan 2024

---

## Abstract

We address the existence, stability, and evolution of two-dimensional vortex quantum droplets (VQDs) in binary Bose-Einstein condensates trapped in a ring-shaped potential. The interplay of the Lee-Huang-Yang-amended nonlinearity and trapping potential supports two VQD branches, controlled by the radius, width and depth of the potential profile. While the lower-branch VQDs, bifurcating from the system's linear modes, are completely unstable, the upper branch is fully stable for all values of the topological charge  $m$  and potential's parameters. Up to  $m = 12$  (at least), stable VQDs obey the *anti-Vakhitov-Kolokolov* criterion. In the limit of an extremely tight radial trap, the modulational instability of the quasi-1D azimuthal VQDs is studied analytically. We thus put forward an effective way to produce stable VQDs with higher vorticity but a relatively small number of atoms, which is favorable for experimental realization.

*Keywords:* Vortex droplets; Quantum fluctuations; Stability.

---

## 1. Introduction

The past few years have witnessed significant advancements in studies of the evolution dynamics of quantum droplets (QDs) [1–6]. QDs draw much interest due to their unique properties. In particular, the quantum liquid of which the QDs are made is eight orders of magnitude more dilute than liquid helium, constituting the most dilute liquid known in physics [3–5]. QDs behave as nearly incompressible self-sustained liquid droplets, with the core featuring a uniform density in the limit of large atom numbers [1]. QDs may be stable not only in their fundamental state, but also in excited forms, e.g., as vortex QDs (VQDs) or multipole-mode QDs in both two-dimensional (2D) [7–9] and three-dimensional (3D) [10, 11] geometries.

The possibility of creating stable QDs in binary Bose-Einstein condensates (BECs) with contact inter-atomic interactions was theoretically predicted by Petrov *et al.* [1, 2], assuming intrinsic self-repulsion in each component and dominating attraction between them, imposed by means of the Feshbach resonance [12]. Further, the attraction-induced collapse is arrested by the self-repulsive correction to the BEC energy resulting from zero-point quantum fluctuations around the mean-field state. The latter was derived by Lee, Huang, and Yang (LHY)

in 1957 [13], and extended to binary mixtures in 1963 [14]. Experimentally, anisotropic QDs were created in dipolar BECs by exploiting the competition between the contact repulsion and dipole-dipole attraction [3, 15–18]. Quasi-2D [5, 19] and full 3D isotropic QDs [20] were observed in mixtures of two different atomic states in  $^{39}\text{K}$  and in an attractive mixture of  $^{41}\text{K}$  and  $^{87}\text{Rb}$  atoms [21], which feature solely contact interactions. QDs in binary dipolar BECs were also reported recently [22, 23].

Theoretical works have confirmed close agreement between properties of QDs predicted by the LHY-amended Gross-Pitaevskii equations (GPEs) and by the many-body theory based on the quantum diffusion Monte-Carlo method [24–29]. Thus, properties of QDs were predicted in the framework of the LHY-amended GPEs in various settings [7–9, 30–44]. In particular, it was predicted that 2D and 3D asymmetric QDs may perform circular motion in an anharmonic trapping potential [45].

Vortices are ubiquitous objects appearing in various branches of nonlinear physics, including BECs, nonlinear optics, classical and quantum hydrodynamics, magnetism, etc. [46]. They can be generated by means of various experimental techniques and have found extensive applications in a variety of fields, such as quantum computing, optical trapping, and superconductors [47]. Specifically, while 2D fundamental QDs in symmetric binary BECs are completely stable, their stable VQDs counterparts can be found with the topological charge up to  $m = 5$ , provided that the VQD's atom number (norm) exceeds a certain

---

\*Corresponding author.

\*\*Sabbatical address.

*Email address:* dlw00@163.com (Liangwei Dong)

critical value [7]. Stable 3D VQDs have been found, thus far, with  $m = 1$  and 2 [10]. Internal modes of stable 2D VQDs were studied in Ref. [8] (see also Ref. [48], where results were reported for intrinsic stability of 2D bound states stabilized by the LHY self-repulsion in the singular trapping potential  $\sim -1/r^2$ ). Binary QDs with heterosymmetric structures in their components were studied too [34]. Metastable globally-linked QD clusters and rotating VQD ones with multiple singly quantized vortices were predicted in symmetric binary BECs [35, 36]. Semidiscrete optical vortex droplets can exist in quasi-phase-matched photonic crystals [49].

In the absence of external trapping, VQDs with high topological charges are stable only for BECs containing an extremely large number of atoms [7, 10]. Then, challenging issues are if it is possible to design a practically relevant setting for the realization of stable VQDs with higher values of the topological charge (e.g.,  $m = 12$ ), if VQDs with large  $m$  may be made stable with relatively small atom numbers, and whether one can control the distribution of VQDs in such settings.

In this paper, we investigate the existence, stability, and dynamics of VQDs in symmetric binary BECs trapped in an annular potential. The analysis reveals that the radius, thickness and depth of the annular potential can be used to control VQD properties. In particular, VQDs belonging to an upper branch of solutions are stable in their entire existence domains. We demonstrate that stable VQDs with higher values of  $m$  can be found for symmetric binary BECs containing relatively small numbers of atoms. In addition to the systematic numerical studies, analytical consideration is performed for the modulational instability (MI) of azimuthally uniform VQDs in the quasi-1D limit of an extremely narrow and deep annular trap. These findings suggest the way for the experimental creation of elusive self-sustained higher-charge 2D vortex droplets in BECs.

## 2. The theoretical model

The evolution of wave functions  $\Psi_{1,2}(x, y, z, t)$  of the two components of the 3D binary BECs is governed by the GPE system with the mean-field cubic terms augmented by the LHY-induced quartic self-repulsion [1]. For the BEC strongly confined in the transverse direction, the full GPE system can be reduced to the 2D system for modes with lateral size  $l \gg \sqrt{a_{1,2}a_{\perp}}$ , where  $a_{1,2}$  and  $a_{\perp}$  are the self-repulsion scattering lengths of the two component and the transverse-confinement length, respectively [50]. Typical parameters relevant to the experiments with the quasi-2D setups, *viz.*,  $l \sim 10 \mu\text{m}$ ,  $a_{1,2} \sim 3 \text{ nm}$  and  $a_{\perp} \lesssim 1 \mu\text{m}$  [1, 2], satisfy this condition. In the scaled form, the effective 2D system is [2]

$$i \frac{\partial \Psi_{1,2}}{\partial t} = -\frac{1}{2} \nabla^2 \Psi_{1,2} + V(x, y) \Psi_{1,2} + \frac{4\pi}{g} (|\Psi_{1,2}|^2 - |\Psi_{2,1}|^2) \Psi_{1,2} + (|\Psi_1|^2 + |\Psi_2|^2) \ln(|\Psi_1|^2 + |\Psi_2|^2) \Psi_{1,2}. \quad (1)$$

where  $\nabla^2 = \partial_{xx} + \partial_{yy}$ ,  $V(x, y)$  is the external potential, and  $g > 0$  is the coupling constant. Further, we focus, as usual, on the symmetric system, with,  $a_1 = a_2$  and  $\Psi_1 = \Psi_2 = \Psi/\sqrt{2}$ .

With the addition rescaling,  $(x, y) \rightarrow (g/2\sqrt{\pi})(x, y)$  and  $t \rightarrow (g^2/4\pi)t$ , the final form of the 2D LHY-amended GPE becomes

$$i \frac{\partial \Psi}{\partial t} = -\frac{1}{2} \nabla^2 \Psi + |\Psi|^2 \ln(|\Psi|^2) \Psi + V(x, y) \Psi. \quad (2)$$

We consider the QD dynamics under the action of an annular potential, defined as

$$V(r) = -p \exp[-(r - r_0)^2/d^2], \quad (3)$$

where  $(r, \theta)$  are the polar coordinates,  $r_0$ ,  $d$ , and  $p$  being the radius, width, and depth of the annular potential. The most relevant case is the one with the potential depth being on the same order of magnitude as the spatial scale corresponding to the nonlinear term in Eq. (2).

Stationary solutions of Eq. (2) with chemical potential  $\mu$  are searched for as  $\Psi(x, y, t) = \psi(x, y) \exp(-i\mu t) \equiv [\psi_r(x, y) + i\psi_i(x, y)] \exp(-i\mu t)$ , where  $\psi_r$  and  $\psi_i$  are the real and imaginary parts of the stationary wave function, whose phase is  $\phi = \arctan(\psi_i/\psi_r)$ . The substitution of this ansatz in Eq. (2) results in a stationary equation

$$\frac{1}{2} \nabla^2 \psi + \mu \psi - V(r) \psi - |\psi|^2 \ln(|\psi|^2) \psi = 0, \quad (4)$$

from which stationary states can be looked for by dint of the relaxation or Newton-conjugate-gradient method [51]. QD families are characterized by the set of parameters  $\mu$ ,  $r_0$ ,  $d$  and  $p$ .

Equation (2) conserves three dynamical invariants, namely, the norm (scaled number of atoms)  $N$ , Hamiltonian (energy)  $E$ , and the total angular momentum  $M_z$ :

$$\begin{aligned} N &= \iint |\Psi|^2 dx dy, \\ E &= \frac{1}{2} \iint \left[ |\nabla \Psi|^2 + 2V|\Psi|^2 + |\Psi|^4 \ln\left(\frac{|\Psi|^2}{\sqrt{e}}\right) \right] dx dy, \\ M_z &= i \iint \left[ \Psi^* \left( y \frac{\partial}{\partial x} - x \frac{\partial}{\partial y} \right) \Psi \right] dx dy \equiv i \iint \Psi^* \frac{\partial}{\partial \theta} \Psi dx dy. \end{aligned} \quad (5)$$

For vortex states with topological charge  $m$ ,  $\Psi(x, y, t) = \psi(x, y) \exp(im\theta - i\mu t)$ , one has  $M_z = mN$ .

The analysis of the QD stability is crucially important for identifying physically relevant states. To this end, one should use the linearized Bogoliubov-de Gennes equations (BdGEs) [52, 53] for small perturbations  $f(x, y)$  and  $g(x, y)$  of the wave functions, defined so that

$$\begin{aligned} \Psi(x, y, t) &= [\psi + f(x, y) \exp(\delta t) \\ &\quad + g^*(x, y) \exp(\delta^* t)] \exp(-i\mu t), \end{aligned} \quad (6)$$

where  $\delta$  is the (generally, complex) growth rate of the perturbation, and  $*$  stands for the complex conjugate. The linearization of Eq. (2) for the small perturbations leads to the linear-stability eigenvalue problem

$$\delta \begin{bmatrix} f \\ g \end{bmatrix} = i \begin{bmatrix} M_1 & M_2 \\ -M_2^* & -M_1^* \end{bmatrix} \begin{bmatrix} f \\ g \end{bmatrix}. \quad (7)$$

Here,  $M_1 = -(1/2)\nabla^2 + V(r) - \mu + 2|\psi|^2 [\ln(|\psi|^2) + 1/2]$  and  $M_2 = \psi^2 [\ln(|\psi|^2) + 1]$ . Equations (7) can be solved numerically by means of the Fourier collocation algorithm [51]. The QD stability is determined by the spectrum of Eqs. (7). QDs are stable only when all eigenvalues  $\delta$  are pure imaginary.

### 3. The quasi-one-dimensional limit (narrow annular trap): analytical results

Before presenting results of the systematic numerical investigation for the VQDs, which are supported by the annular trapping potential in its general form, and their stability, it is relevant to consider the limit case of a very narrow and deep trap, which makes it possible to produce analytical results. In this limit, the narrow radial Gaussian (3), with small  $d$  and large  $p$ , may be approximated as

$$V(r) = p \exp[-(r-r_0)^2/d^2] \approx \varepsilon \delta(r-r_0), \varepsilon \equiv \sqrt{\pi} p d \gg r_0^{-1}, \quad (8)$$

where  $\delta(r-r_0)$  is the delta-function. This trapping potential maintains bound states which are strongly confined in the radial direction, *viz.*,

$$\Psi(r, \theta, t) \approx \sqrt{\varepsilon} \exp\left(-\frac{i}{2}\varepsilon^2 t - \varepsilon|r-r_0|\right) \Phi(\theta, t), \quad (9)$$

where the  $r$ -dependent factor is the normalized wave function of the commonly known 1D bound state supported by the delta-functional trapping potential. The reduced GPE for the azimuthal wave function,  $\Phi(\theta, t)$ , can be derived, as usual [54], by the substitution of the factorized ansatz (9) in the underlying equation (2), multiplying it by the same radial wave function as is present in the ansatz, and finally performing the radial integration. The results is

$$i \frac{\partial \Phi}{\partial t} = -\frac{1}{2r_0^2} \frac{\partial^2 \Phi}{\partial \theta^2} + \frac{\varepsilon}{2} |\Phi|^2 \Phi \ln(e^{-1/8} \varepsilon |\Phi|^2). \quad (10)$$

It is relevant to stress that the effective 1D equation (10) keeps the 2D form of the nonlinear term in the case when the radial-localization range,  $\sim 1/\varepsilon$  in Eq. (9) (which is on the order of  $\mu\text{m}$ , in experimentally relevant settings), is much smaller than  $r_0$ , but large in comparison to the underlying healing length, which is typically  $\xi \sim 30\text{ nm}$  [5, 19–21]. In the limit of the extremely tight-confinement range, which is smaller than the healing length, the LHY correction to the effective 1D GPE is different, being represented by the self-attractive quadratic term,  $\sim |\Phi|\Phi$  [2]. In particular, the MI of spatially uniform states, which is the central issue of the analytical consideration presented in this section, was analyzed, in the framework of the latter model, in Refs. [55–57].

Getting back to Eq. (10), which is the experimentally relevant model in the present context, its azimuthally uniform solutions with amplitude  $A$ , carrying integer vorticity  $m$ , are

$$\begin{aligned} \Phi &= A \exp(-i\mu t + im\theta), \\ \mu &= \frac{m^2}{2r_0^2} + \frac{\varepsilon}{2} A^2 \ln(e^{-1/8} \varepsilon A^2). \end{aligned} \quad (11)$$

In terms of the quasi-1D limit, the instability of the higher-order VQD states, with large values of  $m$ , corresponds to the MI of solutions (11) in the framework of Eq. (10). The Galilean invariance of this equation implies that the stability does not depend on  $m$ , which helps to understand the fact that the VQD stability, analyzed below in terms of the full 2D model (2), readily extends to solutions with large values of  $m$ .

Thus, the MI of solutions (11) depends solely on their amplitude  $A$ . The straightforward analysis, which takes into regard the “quantization” of wavenumbers of the modulational perturbations, which may assume only integer values,  $p = \pm 1, \pm 2, \dots$ , leads to the following MI condition:

$$A^2 \ln(e^{7/8} \varepsilon A^2) < -p^2 / (2r_0^2 \varepsilon). \quad (12)$$

Further, the analysis of condition (12) demonstrates that this condition *does not hold* for all  $p^2 \geq 1$ , provided that the radius of the narrow trapping potential is not too large, *viz.*,

$$r_0 \leq e^{15/16} / \sqrt{2} \approx 1.8. \quad (13)$$

Thus, condition (13) guarantees the full stability of all vortex states in the framework of the quasi-1D limit (10).

### 4. Numerical results

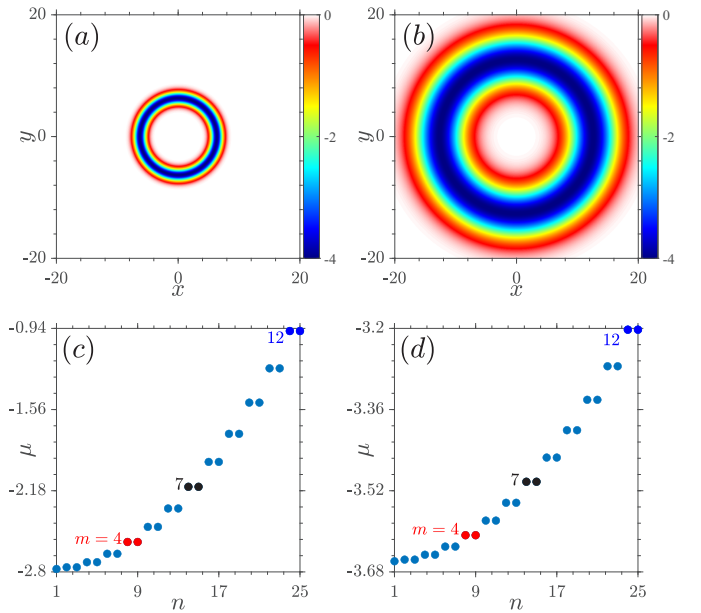


Fig. 1. Examples of the annular potential (3) with  $r_0 = 2\pi, d = 1$  (a) and  $r_0 = 4\pi, d = 4$  (b). (c,d) Spectra of eigenvalues  $\mu$  of the linearized equation (4) for the potentials shown in (a) and (b), respectively. Labels  $m$  denotes eigenvalues from which VQDs with topological charges  $m = 4, 7$  and  $12$  bifurcate. In all the panels, the potential depth is  $p = 4$ .

To explore effects of the radius and width of the ring-shaped potential (3) on the QDs, we fix the potential’s depth as  $p = 4$  and vary its radius  $r_0$  and width  $d$ . Two representative examples of the potential are presented in Figs. 1(a,b). Note that the

potential is symmetric about the central circle with  $r = r_0$ , i.e.,  $V(r = r_0 - r') = V(r = r_0 + r')$ , for all  $0 < r' < r_0$ . This symmetry implies the same guidance for the wave function in the inner and outer annuli ( $r < r_0$  and  $r > r_0$ , respectively), unlike the case of the harmonic-oscillator (HO) trapping potential, which is commonly used to trap BEC and guide optical beams. We have found that the potential defined by Eq. (3) suppresses the instability of vortex solitons with high values of the topological charge which is known in the case of the HO trapping potential [58]. Stable higher-order solitons with a multiring profile are also expected to be maintained by potential (3).

Before addressing the VQDs in the nonlinear regime, it is instructive to produce the dispersion relation of the linear system with the same potential (3). The nonlinearity results in bifurcations of nonlinear modes from different linear eigenstates, at respective eigenvalues. The spectrum of the linear version of Eq. (4) is composed of a series of discrete eigenvalues [Figs. 1(c,d)], supplemented by continuous spectrum (not shown here), in contrast to the system with the HO potential, in which case the discrete eigenvalues are distributed evenly.

The linear spectrum is determined by parameters of the trapping potential. The variation of radius  $r_0$ , width  $d$ , and depth  $p$  shift the spectrum and alter the distribution of the eigenvalues in the spectrum on the other. While fundamental QDs bifurcate from the eigenmode corresponding to the first eigenvalue, dipole droplets bifurcate from the eigenmodes corresponding to the second and third (mutually degenerate) eigenvalues. The linear dipole modes corresponding to the second and third eigenvalues are mutually perpendicular. For topological charge  $m$ , one can obtain droplets with  $2m$  poles from the eigenmodes corresponding to the eigenvalues with numbers  $n = 2m$  and  $2m + 1$ .

In addition to the fundamental and multipole droplets, VQDs can also bifurcate from linear superpositions of two degenerate modes. For example, VQDs with  $m = \pm 1$  bifurcate from linear modes  $\Psi_{\pm 1} = \Psi_{1,2} \pm i\Psi_{1,3}$ , where the first and second subscripts refer to the topological charge and serial number of the basic eigenmodes, respectively. More generally, VQDs with topological charge  $m$  bifurcate from the superposition of the pair of mutually degenerate linear modes  $\Psi_{\pm m} = \Psi_{m,2m} \pm i\Psi_{m,2m+1}$ , which correspond to the same  $2m$ -th eigenvalue.

It is known that, in the framework of Eq. (2) in the free space ( $V = 0$ ), VQDs in the 2D symmetric binary BEC can be stable with topological charge up to  $m = 5$  (at least), provided that the atom number (norm) exceeds a critical value [7, 8]. To demonstrate the stabilization effect of annular potentials on VQDs with higher charges, in Fig. 2 we produce several representative examples of stable VQDs with  $m = 7$  in the potential (3) with  $r_0 = 2\pi, d = 1$  and  $r_0 = 4\pi, d = 1$  (recall  $p = 4$  is fixed). They exhibit a ring-shaped profile of  $|\psi(r)|$  distribution, resembling the shape of the trapping potential, cf. Figs. 1(a,b). The amplitude and thickness of the VQDs change with the variation of chemical potential  $\mu$ . The radius at which  $|\psi(r)|$  attains its maximum is naturally constrained by radius  $r_0$  of the annular potential. This fact indicates that VQDs are strongly shaped by the trapping potential, in contrast to the flat-top profiles of the free-space VQDs and vortex solitons in optical media with

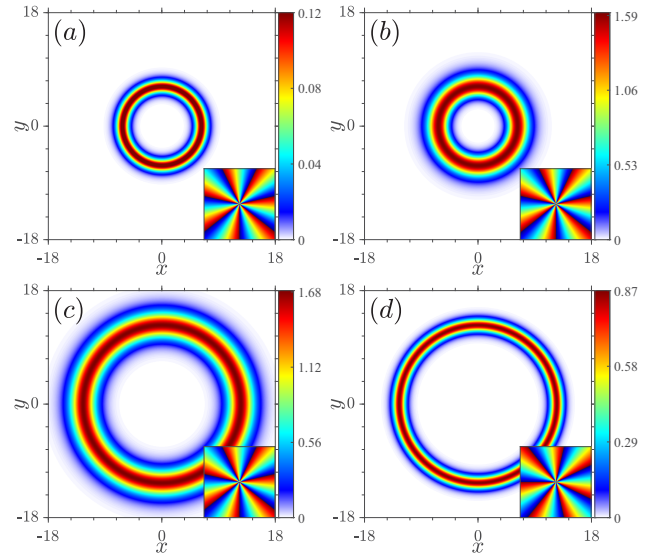


Fig. 2. Profiles of  $|\psi(r)|$  for VQDs with  $m = 7$ , marked in Fig. 3(a), in the annular potentials (3) with  $r_0 = 2\pi, d = 1$  (a,b) and  $r_0 = 4\pi, d = 1$  (c,d). The chemical potential is  $\mu = -2.2$  in (a),  $-0.5$  in (b,c), and  $-2.9$  in (d). Insets: the corresponding phase structures. The vortex shown in (a) belongs to the lower branch, and ones (b-d) belong to the upper branch. In all the panels, the potential's depth is  $p = 4$ .

competing nonlinearities, cf. Refs. [7, 8, 59].

Another essential difference from the free-space VQDs is the fact that the presence of the annular potential makes the norm (scaled atom number)  $N$  of VQDs a nonmonotonous function of the chemical potential, as shown in Fig. 3(a). First,  $N$  increases first with the decrease of  $\mu$ , under the action of the effective attractive nonlinearity in Eq. (4) in the case of  $|\psi| < 1$ . The increase of  $N$  is accompanied by the increase of the droplet's amplitude,  $|\psi|_{\max}$ , and its expansion, see Figs. 3(c,d). In the case of  $|\psi| > 1$ , the logarithmic factor switches the sign of the nonlinearity to the repulsion. The further increase of  $N$  accelerates the growth rate of the effective droplet's width, defined by relation

$$W^2 = N^{-1} \iint (x^2 + y^2) \psi^2 dx dy,$$

as seen in Fig. 3(d), and slows down the growth rate of  $|\psi|_{\max}$  in Fig. 3(c).

In the interplay with the trapping potential, the switch of the attractive interaction into repulsive prevents the existence of the VQD branch with  $dN/d\mu < 0$  to the left of the cutoff point, i.e., at  $\mu < \mu_{\text{cut}}$ . As seen in Fig. 3(a), at the cutoff point the terminating lower VQD branch merges with the upper one, with the same vorticity  $m$  but opposite sign of the slope,  $dN/d\mu > 0$ . The upper branch is dominated by the nonlinearity with the repulsive sign.

For the comparison's sake, Fig. 3(a) also includes the  $N(\mu)$  dependences for the VQD families with  $m = 4$  and  $12$  in the annular potentials with  $r_0 = 2\pi, d = 1$  and  $r_0 = 4\pi, d = 1$ . The VQDs with different values of  $m$  bifurcate from combinations of linear mutually degenerate states at the corresponding



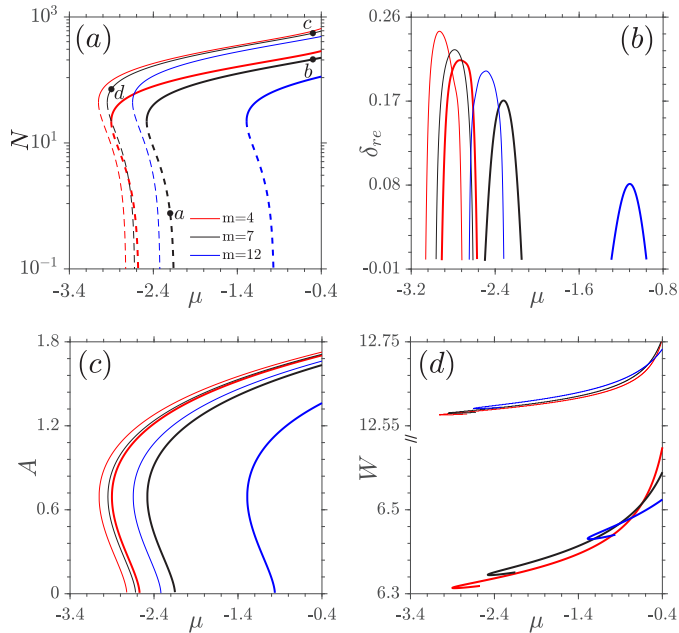


Fig. 3. (a) Norm  $N$  vs. chemical potential  $\mu$  for VQDs with  $m = 4, 7$  and  $12$ . Solid and dashed segments designate stable and unstable states, respectively. (b) The instability growth rate  $\delta_{re} \equiv \text{Re}(\delta)$  vs.  $\mu$  for the VQD solutions belonging to the lower branches of the  $N(\mu)$  families. (c,d) The amplitude  $A \equiv |\psi|_{\max}$  and width of the VQDs with  $m = 4, 7$  and  $12$  versus  $\mu$ . In all the panels, the potential's depth is  $p = 4$ . The data for the VQDs with  $m = 4, 7$  and  $12$  are shown by red, black and blue curves, respectively. The thick and thin lines correspond to the potential with  $r_0 = 2\pi$  and  $4\pi$ . In both cases, the potential's width is  $d = 1$ .

eigenvalues. Specifically, in the potential with  $r_0 = 2\pi, d = 1$  the VQDs with  $m = 4, 7$  and  $12$  bifurcate, severally, from  $\mu = -2.571, -2.149$ , and  $-0.960$  [these bifurcation points are marked in Fig. 1(c)]. The bifurcation values of  $\mu$  for the VQDs in the potential with  $r_0 = 4\pi, d = 1$  are  $-2.725$  (for  $m = 4$ ),  $-2.619$  ( $m = 7$ ), and  $-2.318$  ( $m = 12$ ). It is obvious that the  $N(\mu)$  dependences are very similar for the VQDs with different vorticities  $m$  in the potentials with different widths  $d$  are similar to each other. The increase of the potential's radius shifts the norm curves leftward. The value of the norm at the cut-off (branch-merger) point in the potential with a larger radius ( $r_0 = 4\pi$ ) is higher than in the case of the smaller small radius ( $r_0 = 2\pi$ ).

The central finding of this paper is that the annular potential added to the LHY-amended GPE helps to stabilize VQDs with  $m > 5$ . To illustrate this point, we have conducted linear stability analysis of the obtained stationary VQD solutions, based on BdGEs (7). The smaller amplitude  $|\psi|_{\max}$  of the lower-branch VQD solutions makes the self-attraction a dominant term, leading to the splitting instability of the vortex modes, driven by the MI of the axisymmetric ring-shaped modes against azimuthal perturbations. Indeed, the numerical solution of Eqs. (7) yields nonzero instability growth rates for the lower-branch VQDs with different vorticities  $m \neq 0$ , in the annular potentials (3)

with both  $r_0 = 2\pi$  and  $4\pi$  [Fig. 3(b)].

Note that the negative slope of the lower branch  $N(\mu)$  of the VQD solutions,  $dN/d\mu < 0$ , implies that this branch satisfies the well-known Vakhitov-Kolokolov (VK) necessary stability condition, which actually implies the absence of pure real unstable eigenvalues produced by the BdGEs [60, 61]. However, the splitting instability is not comprised by the VK criterion, as it is accounted for by complex unstable eigenvalues [61–63].

On the other hand, the numerical solutions of BdGEs (7) produces the full spectrum of eigenvalues with  $\text{Re}(\sigma) = 0$  in their whole existence domain, regardless of the values of potential's width, radius, and depth. This result indicates that the upper-branch VQD families are completely stable. As concerns the respective  $N(\mu)$  dependences, which feature  $dN/d\mu > 0$  in Fig. 3(a), they comply with the anti-VK stability criterion [64], which is precisely  $dN/d\mu > 0$  in the case when bound states are maintained by the self-repulsive nonlinearity.

We stress that the stable upper-branch VQD solutions feature a relatively small number of atoms. In particular, the stability conditions for the vortices with  $m = 7$  in the trapping potential (3) with  $r_0 = 2\pi, d = 1$ , or  $r_0 = 4\pi, d = 1$  are, respectively,  $N \geq 21.95$  or  $N \geq 43.91$ . This is in sharp contrast to the case without the trapping potential, where the stability conditions for the VQDs with  $m = 2$  or  $m = 5$  are, severally,  $N \geq 200$  or  $N \geq 3550$  [7]. The VQD norm in the free space dramatically increases, featuring  $N \rightarrow \infty$ , as  $\mu$  is approaching the upper cut-off. For instance, the chemical potential of the  $m = 5$  VQD with  $N = 3550$  is  $\mu = -0.297$ , which is close to the respective cut-off point,  $\mu_{\text{cut}} = -0.304$  [8]. Thus, the addition of the annular trapping potential to the LHY-amended BEC model drastically reduces the number of atoms required for the creation of stable higher-order VQDs, making it much easier to realize the predictions in the experiments.

The dependence of the amplitude,  $|\psi|_{\max}$ , of the VQDs with different vorticities, trapped in the annular potentials with different thicknesses, on the chemical potential  $\mu$  is shown in Fig. 3(c). At first, the amplitude increases with the decrease of  $\mu$ . Passing the turning (cutoff) point, it keeps increases with the subsequent growth of  $\mu$ , although slower. At fixed  $\mu$ , the effective width of the VQDs in the trapping potential with  $r_0 = 4\pi$  is approximately twice that in the potential with  $r_0 = 2\pi$ , see Fig. 3(d). This finding again confirms that the VQDs are confined within the ring potential. Adjusting the potential's radius, one can create VQDs with any desired radius.

To study the stability of VQDs with high topological charges, we consider them with  $m = 1$  to  $12$  in setups with different parameters of the annular potential (3). For illustration, in Figs. 4(a,b) we present the profiles of  $|\psi|$  of two VQDs with  $m = 12$  at different values of  $\mu$  in the annular potential with  $r_0 = 4\pi$  and  $d = 4$ . The vortex is thin at large  $|\mu|$  and thick at small  $|\mu|$ . Due to the strong repulsive nonlinearity and the confinement imposed by the annular potential, with the increase of  $\mu$ , the VQD demonstrates symmetric expansion with respect to the central circle (where the potential attains its maximum). The dependence  $N(\mu)$  for VQDs with vorticities  $m = 4, 7$  and  $12$  is shown in Fig. 4(c). The bifurcation points at which the VQDs emerge from the linear modes are  $\mu = -3.607, -3.502$ , and

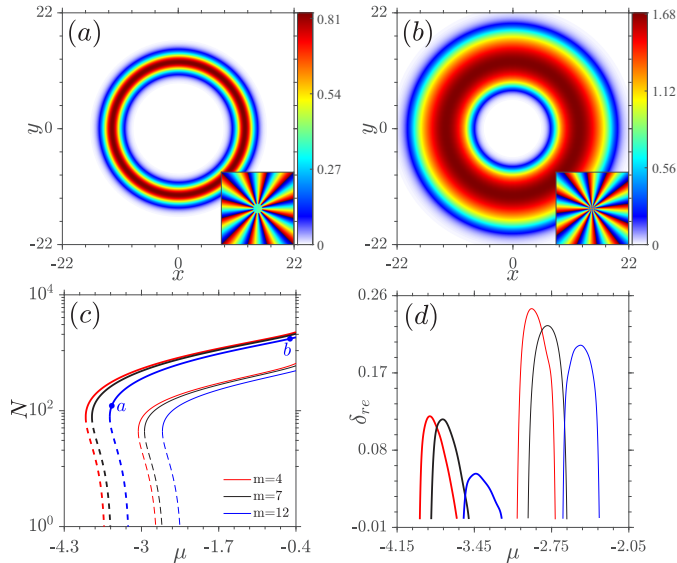


Fig. 4. Examples of the upper-branch VQDs with  $m = 12$  marked in (c) at  $\mu = -3.5$  (a) and  $-0.5$  (b), in the trapping potential (3) with  $r_0 = 4\pi$  and  $d = 4$ . (c) Norm  $N$  vs.  $\mu$  for the VQDs with  $m = 4, 7$  and  $12$ . Solid and dashed curves depict stable and unstable subfamilies, respectively. (d) The stability growth rate  $\delta_{re} \equiv \text{Re}(\delta)$  vs.  $\mu$  for the lower-branch VQDs (the red, black, and blue branches represent  $m = 4, 7$ , and  $12$ , respectively). The thick and thin lines correspond to the annular potential with  $r_0 = 4\pi, d = 4$  and  $r_0 = 4\pi, d = 1$ , respectively. In all the cases, the potential's depth is  $p = 4$ .

$-3.202$  for  $m = 4, 7$  and  $12$ , respectively. The norm remains a nonmonotonous function of  $\mu$ , similar to the  $N(\mu)$  curves shown in Fig. 3(a). The growth of the potential's width  $d$  leads to an increase of the critical values of  $N$  at the turning points, where the lower and upper branches merge. The growth of  $d$  also shifts the  $N(\mu)$  curve leftward.

The stability analysis results shown in Fig. 4(d) demonstrate that, as said above, all VQDs belonging to the lower branches (with  $dN/d\mu < 0$ ) are unstable. Yet, the instability growth rate for these solutions decreases with the increase of width  $d$  of the annular trapping potential (3). As a result, one can obtain nearly stable VQDs belonging to the lower branch, with small atom numbers.

The complete stability region of the upper-branch VQDs is in sharp contrast to that for the upper-branch VQDs trapped in the HO potential [65], where the stability region quickly shrinks with the growth of the vorticity.

Although we have displayed in detail the examples of VQDs with  $m = 4, 7$  and  $12$ , our main results hold as well for all VQDs with even and odd vorticity, at least for  $m \leq 12$ . The properties of VQDs also remain qualitative unchanged for varying potential depths  $p$ . It is plausible that the upper-branch VQDs remain stable for even higher values of  $m$ . We have also checked the stability of the fundamental QDs with  $m = 0$  in the annular potentials, concluding that the fundamental QDs belonging to the corresponding lower branch remain unstable for all values of the parameters of the annular trapping potential. As well

as the lower-branch vortex modes, this is the azimuthal MI, as confirmed by direct simulations below, see Figs. 5(e-l).

To validate the predictions of the linear-stability analysis, we have performed extensive evolution simulations of VQDs with different topological charges in the trapping potential with various parameters, by means of the split-step Fourier method with absorptive boundary condition. The perturbation was added, as white noise in the form  $\Psi(x, y, t = 0) = \psi(x, y)[1 + \rho(x, y)]$ , to the input at  $t = 0$  for the stable VQDs and no noise was added to the unstable droplets, whose instability was predicted by the computation of eigenvalues for small perturbations. For unstable VQDs, the random perturbation was taken with variance  $\sigma_{\text{noise}} = 0.01$ .

Typical examples of the simulated perturbed solutions are displayed in Fig. 5. In particular, the inputs used in panels (b) and (c) correspond to the stationary VQDs shown in Figs. 2(b) and 4(b), respectively. The upper-branch VQDs which are predicted to be stable indeed preserve their amplitude and phase structures in the course of arbitrarily long simulations, as shown in Figs. 5(a-d). On the other hand, the unstable lower-branch VQDs spontaneously break up into one or several azimuthal fragments after a short evolution time. To further highlight the instability of the lower-branch VQDs, we present examples for the fundamental droplet (with  $m = 0$ ) in Figs. 5(e-h) and for the VQD ( $m = 12$ ) in Figs. 5(i-l). As previously stated, the direct simulations clearly demonstrate that the onset of the azimuthal MI occurs.

## 5. Conclusion

In this work we have investigated the stability and dynamics of VQDs (vortex quantum droplets) in the 2D symmetric binary BEC trapped in the annular potential. Two branches of the VQD solutions, with opposite slopes of the norm-vs.-chemical-potential curves, are supported by the mean-field nonlinearity amended by the LHY (Lee-Hung-Yang) correction, i.e., the cubic term times the logarithmic factor. Although the profiles of VQDs vary with the chemical potential and topological charge  $m$ , they are confined by the trapping potential, providing a new way to control their radius, width, and amplitude. While the lower-branch VQDs, bifurcating from the linear modes, are unstable in their entire existence domain, the upper branch is completely stable, for all values of  $m$  and potential's parameters. The stability of the upper-branch VQDs with  $m \leq 12$  (at least), for which the effective nonlinearity is self-repulsive, agrees with the *anti-Vakhitov-Kolokolov* criterion. We have also produced analytical results for the MI (modulational instability) of quasi-1D VQDs, trapped in an extremely tight annular potential. The findings propose an effective way for the creation of stable higher-order vortex droplets with a relatively small number of atoms, which is favorable for the experimental realization.

### CRedit authorship contribution statement

Liangwei Dong: Conceptualization and writing the original draft; Mingjing Fan: Numerical calculations; Boris A. Malomed: Analytical investigation, writing, review & editing and

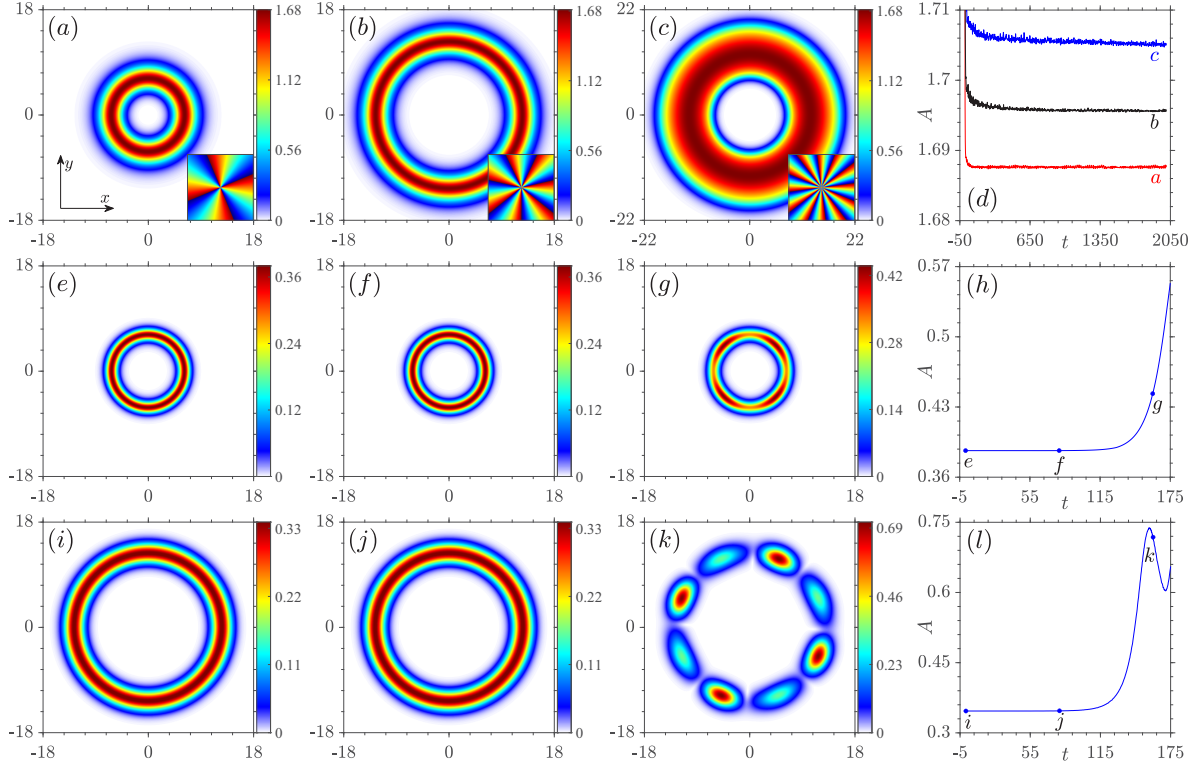


Fig. 5. (a-c) Vortex profiles with  $m = 4, 7$  and  $12$  marked in (d) at  $t = 2000$ . The potential parameters  $r_0 = 2\pi, d = 1$  in (a),  $r_0 = 4\pi, d = 1$  in (b) and  $r_0 = 4\pi, d = 4$  in (c). Insets: the corresponding phase patterns. (d) Dependence of peak amplitudes  $A = \max|\Psi(t)|$  of stable upper-branch vortex droplets on  $t$ . The blue curve is increased by  $0.01$  to avoid the overlaps with the black curve. The chemical potential  $\mu = -0.5$  in (a-d). (e-f) Unstable evolution of the lower-branch fundamental droplet marked in (h) at  $\mu = -3$  in the potential with  $r_0 = 2\pi, d = 1$ . (h) Peak amplitude  $\max|\Psi(t)|$  of the unstable fundamental droplet shown in (e) versus  $t$ . (i-k) Unstable evolution of the lower-branch VQD with  $m = 12$  marked in (l) at  $\mu = -3.4$  in the potential with  $r_0 = 4\pi, d = 4$ . (h) Peak amplitude  $\max|\Psi(t)|$  of the unstable vortex shown in (i) versus  $t$ .

validation.

**Declaration of competing interest** The authors declare the following financial interests/personal relationships which may be considered as potential competing interests: Liangwei Dong reports financial support provided by Natural Science Basic Research Program in Shaanxi Province of China (grant No. 2022JZ-02); Boris A. Malomed reports financial support provided by the Israel Science Foundation through grant No. 1695/22.

**Data availability** Data will be made available on request.

**Acknowledgements** This work is supported by the Natural Science Basic Research Program of Shaanxi Province of China (Grant No. 2022JZ-02) and Israel Science Foundation (Grant No. 1695/22).

## References

- [1] D. S. Petrov, Quantum mechanical stabilization of a collapsing Bose-Bose mixture, *Phys. Rev. Lett.* 115 (2015) 155302.
- [2] D. S. Petrov, G. E. Astrakharchik, Ultradilute low-dimensional liquids, *Phys. Rev. Lett.* 117 (2016) 100401.
- [3] M. Schmitt, M. Wenzel, F. Böttcher, I. Ferrier-Barbut, T. Pfau, Self-bound droplets of a dilute magnetic quantum liquid, *Nature* 539 (2016) 259.
- [4] Y. V. Kartashov, V. V. Konotop, D. A. Zezyulin, L. Torner, Bloch oscillations in optical and zeeman lattices in the presence of spin-orbit coupling, *Phys. Rev. Lett.* 117 (2016) 215301.
- [5] C. R. Cabrera, L. Tanzi, J. Sanz, N. Naylor, P. Thomas, P. Cheiney, T. L., Quantum liquid droplets in a mixture of Bose-Einstein condensates, *Science* 359 (2018) 301.
- [6] I. Ferrier-Barbut, Ultradilute quantum droplets, *Phys. Today* 72 (2019) 46.
- [7] Y. Li, Z. Chen, Z. Luo, C. Huang, H. Tan, W. Pang, B. A. Malomed, Two-dimensional vortex quantum droplets, *Phys. Rev. A* 98 (2018) 063602.
- [8] L. Dong, K. Shi, C. Huang, Internal modes of two-dimensional quantum droplets, *Phys. Rev. A* 106 (2022) 053303.
- [9] L. Dong, D. Liu, Z. Du, K. Shi, W. Qi, Bistable multipole quantum droplets in binary Bose-Einstein condensates, *Phys. Rev. A* 105 (2022) 033321.
- [10] Y. V. Kartashov, B. A. Malomed, L. Tarruell, L. Torner, Three-dimensional droplets of swirling superfluids, *Phys. Rev. A* 98 (2018) 013612.
- [11] L. Dong, M. Fan, Stable higher-charge vortex droplets governed by quantum fluctuations in three dimensions, *Chaos Solitons Fractals* 173 (2023) 113728.
- [12] G. Roati, M. Zaccanti, C. D'Errico, J. Catani, M. Modugno, A. Simoni, M. Inguscio, G. Modugno,  $^{39}\text{K}$  Bose-Einstein condensate with tunable interactions, *Phys. Rev. Lett.* 99 (2007) 010403.
- [13] T. D. Lee, K. Huang, C. N. Yang, Eigenvalues and eigenfunctions of a Bose system of hard spheres and its low-temperature properties, *Phys. Rev.* 106 (1957) 1135–1145.
- [14] D. M. Larsen, Binary mixtures of dilute Bose gases with repulsive interactions at low temperature, *Annals of Physics* 24 (1963) 89–101.



- [15] H. Kadau, M. Schmitt, M. Wenzel, C. Wink, T. Maier, I. Ferrier-Barbut, T. Pfau, Observing the rosenweig instability of a quantum ferrofluid, *Nature* 530 (2016) 194.
- [16] I. Ferrier-Barbut, H. Kadau, M. Schmitt, M. Wenzel, T. Pfau, Observation of quantum droplets in a strongly dipolar Bose gas, *Phys. Rev. Lett.* 116 (2016) 215301.
- [17] L. Chomaz, S. Baier, D. Petter, M. J. Mark, F. Wächtler, L. Santos, F. Ferlaino, Quantum-fluctuation-driven crossover from a dilute Bose-Einstein condensate to a macrodroplet in a dipolar quantum fluid, *Phys. Rev. X* 6 (2016) 041039.
- [18] G. Li, X. Jiang, B. Liu, Z. Chen, B. A. Malomed, Y. Li, Two-dimensional anisotropic vortex quantum droplets in dipolar Bose-Einstein condensates, *Front. Phys.* 19 (2024) 22202.
- [19] P. Cheiney, C. R. Cabrera, J. Sanz, B. Naylor, L. Tanzi, L. Tarruell, Bright soliton to quantum droplet transition in a mixture of Bose-Einstein condensates, *Phys. Rev. Lett.* 120 (2018) 135301.
- [20] G. Semeghini, G. Ferioli, L. Masi, C. Mazzinghi, L. Wolswijk, F. Minardi, M. Modugno, G. Modugno, M. Inguscio, M. Fattori, Self-bound quantum droplets of atomic mixtures in free space, *Phys. Rev. Lett.* 120 (2018) 235301.
- [21] C. D'Errico, A. Burchianti, M. Prevedelli, L. Salasnich, F. Ancilotto, M. Modugno, F. Minardi, C. Fort, Observation of quantum droplets in a heteronuclear bosonic mixture, *Phys. Rev. Research* 1 (2019) 033155.
- [22] R. N. Bisset, L. A. Peña Ardila, L. Santos, Quantum droplets of dipolar mixtures, *Phys. Rev. Lett.* 126 (2021) 025301.
- [23] J. C. Smith, D. Baillie, P. B. Blakie, Quantum droplet states of a binary magnetic gas, *Phys. Rev. Lett.* 126 (2021) 025302.
- [24] V. Cikojević, L. V. Markić, G. E. Astrakharchik, J. Boronat, Universality in ultradilute liquid Bose-Bose mixtures, *Phys. Rev. A* 99 (2019) 023618.
- [25] V. Cikojević, L. V. Markić, J. Boronat, Finite-range effects in ultradilute quantum drops, *New J. Phys.* 22 (2020) 053045.
- [26] L. Parisi, G. E. Astrakharchik, S. Giorgini, Liquid state of one-dimensional Bose mixtures: A quantum Monte Carlo study, *Phys. Rev. Lett.* 122 (2019) 105302.
- [27] F. Cinti, A. Cappellaro, L. Salasnich, T. Macrì, Superfluid filaments of dipolar bosons in free space, *Phys. Rev. Lett.* 119 (2017) 215302.
- [28] A. Macia, J. Sánchez-Baena, J. Boronat, F. Mazzanti, Droplets of trapped quantum dipolar bosons, *Phys. Rev. Lett.* 117 (2016) 205301.
- [29] V. Cikojević, K. Dželalija, P. Stipanović, L. Vranješ Markić, J. Boronat, Ultradilute quantum liquid drops, *Phys. Rev. B*(R) 97 (2018) 140502.
- [30] G. E. Astrakharchik, B. A. Malomed, Dynamics of one-dimensional quantum droplets, *Phys. Rev. A* 98 (2018) 013631.
- [31] Z. Zhou, X. Yu, Y. Zou, H. Zhong, Dynamics of quantum droplets in a one-dimensional optical lattice, *Commun. Nonlinear Sci. Numer. Simulat.* 78 (2019) 104881.
- [32] J. Chen, J. Zeng, One-dimensional quantum droplets under space-periodic nonlinear management, *Results Phys.* 21 (2021) 103781.
- [33] Z. Zhou, Y. Shi, S. Tang, H. Deng, H. Wang, X. He, H. Zhong, Controllable dissipative quantum droplets in one-dimensional optical lattices, *Chaos Solitons Fractals* 150 (2021) 111193.
- [34] Y. V. Kartashov, B. A. Malomed, L. Torner, Structured heterosymmetric quantum droplets, *Phys. Rev. Research* 2 (2020) 033522.
- [35] Y. V. Kartashov, B. A. Malomed, L. Torner, Metastability of quantum droplet clusters, *Phys. Rev. Lett.* 122 (2019) 193902.
- [36] M. N. Tengstrand, P. Stürmer, E. O. Karabulut, S. M. Reimann, Rotating binary Bose-Einstein condensates and vortex clusters in quantum droplets, *Phys. Rev. Lett.* 123 (2019) 160405.
- [37] X. Zhang, X. Xu, Y. Zheng, Z. Chen, B. Liu, C. Huang, B. A. Malomed, Y. Li, Semidiscrete quantum droplets and vortices, *Phys. Rev. Lett.* 123 (2019) 133901.
- [38] Y.-Y. Zheng, S.-T. Chen, Z.-P. Huang, S.-X. Dai, B. Liu, Y.-Y. Li, S.-R. Wang, Quantum droplets in two-dimensional optical lattices, *Front. Phys.* 16 (2021) 1–10.
- [39] X. Jiang, Y. Zeng, Y. Ji, B. Liu, X. Qin, Y. Li, Vortex formation and quench dynamics of rotating quantum droplets, *Chaos Solitons Fractals* 161 (2022) 112368.
- [40] H. Huang, H. Wang, M. Chen, C. S. Lim, K.-C. Wong, Binary-vortex quantum droplets, *Chaos Solitons Fractals* 158 (2022) 112079.
- [41] Z. Zhao, G. Chen, B. Liu, Y. Li, Discrete vortex quantum droplets, *Chaos Solitons Fractals* 162 (2022) 112481.
- [42] H. Huang, H. Wang, G. Chen, M. Chen, C. S. Lim, K.-C. Wong, Stable quantum droplets with higher-order vortex in radial lattices, *Chaos Solitons Fractals* 168 (2023) 113137.
- [43] S.-L. Xu, Y.-B. Lei, J.-T. Du, Y. Zhao, R. Hua, J.-H. Zeng, Three-dimensional quantum droplets in spin-orbit-coupled Bose-Einstein condensates, *Chaos Solitons Fractals* 164 (2022) 112665.
- [44] Z.-H. Luo, W. Pang, B. Liu, Y.-Y. Li, B. A. Malomed, A new form of liquid matter: Quantum droplets, *Front. Phys.* 16 (2021) 1–21.
- [45] L. Dong, Y. V. Kartashov, Rotating multidimensional quantum droplets, *Phys. Rev. Lett.* 126 (2021) 244101.
- [46] L. M. Pismen, Vortices in nonlinear fields: from liquid crystals to superfluids, from non-equilibrium patterns to cosmic strings, Clarendon Press, Oxford, 1999.
- [47] Y. Shen, X. Wang, Z. Xie, C. Min, X. Fu, Q. Liu, M. Gong, X. Yuan, Optical vortices 30 years on: OAM manipulation from topological charge to multiple singularities, *Light Sci. Appl.* 8 (2019) 90.
- [48] E. Shamriz, Z. Chen, B. A. Malomed, Suppression of the quasi-two-dimensional quantum collapse in the attraction field by the Lee-Huang-Yang effect, *Phys. Rev. A* 101 (2020) 063628.
- [49] X. Xu, F. Zhao, J. Huang, H. He, L. Zhang, Z. Chen, Z. Nie, B. A. Malomed, Y. Li, Semidiscrete optical vortex droplets in quasi-phase-matched photonic crystals, *Opt. Express* 31 (2023) 38343–38354.
- [50] Y. Li, Z. Luo, Y. Liu, Z. Chen, C. Huang, S. Fu, H. Tan, B. A. Malomed, Two-dimensional solitons and quantum droplets supported by competing self- and cross-interactions in spin-orbit-coupled condensates, *New J. Phys.* 19 (2017) 113043.
- [51] J. Yang, *Nonlinear Waves in Integrable and Nonintegrable Systems*, SIAM, Philadelphia, 2010.
- [52] L. P. Pitaevskii, S. Stringari, *Bose-Einstein Condensation*, Oxford University Press, Oxford, UK, 2003.
- [53] C. J. Pethick, H. Smith, *Bose-Einstein Condensation in Dilute Gases*, Cambridge University Press, Cambridge, UK, 2008.
- [54] L. Salasnich, A. Parola, L. Reatto, Effective wave equations for the dynamics of cigar-shaped and disk-shaped Bose condensates, *Phys. Rev. A* 65 (2002) 043614.
- [55] T. Mithun, A. Maluckov, K. Kasamatsu, B. A. Malomed, A. Khare, Modulational instability, inter-component asymmetry, and formation of quantum droplets in one-dimensional binary Bose gases, *Symmetry* 12 (2020) 174.
- [56] C. B. Tabi, S. Veni, E. Wamba, T. C. Kofané, Modulational instability and droplet formation in Bose-Bose mixtures with Lee-Huang-Yang correction and polaron-like impurity, *Phys. Lett. A* 485 (2023) 129087.
- [57] S. R. Otajonov, E. N. Tsoy, F. K. Abdullaev, Modulational instability and quantum droplets in a two-dimensional Bose-Einstein condensate, *Phys. Rev. A* 106 (2022) 033309.
- [58] L. Dong, M. Fan, B. A. Malomed, Stable higher-charge vortex solitons in the cubic-quintic medium with a ring potential, *Opt. Lett.* 48 (2023) 4817–4820.
- [59] V. I. Berezhiani, V. Skarka, N. B. Aleksić, Dynamics of localized and non-localized optical vortex solitons in cubic-quintic nonlinear media, *Phys. Rev. E* 64 (2001) 057601.
- [60] N. G. Vakhitov, A. A. Kolokolov, Stationary solutions of the wave equation in the medium with nonlinearity saturation, *Radiophys. Quant. El+* 16 (1973) 783–789.
- [61] L. Bergé, Wave collapse in physics: principles and applications to light and plasma waves, *Phys. Rep.* 303 (1998) 259–370.
- [62] R. L. Pego, H. A. Warchall, Spectrally stable encapsulated vortices for nonlinear Schrödinger equations, *J. Nonlinear Sci.* 12 (2002) 347–394.
- [63] B. A. Malomed, *Multidimensional solitons*, AIP Publishing: Melville, NY, 2022.
- [64] H. Sakaguchi, B. A. Malomed, Solitons in combined linear and nonlinear lattice potentials, *Phys. Rev. A* 81 (2010) 013624.
- [65] D. Liu, Y. Gao, D. Fan, L. Zhang, Higher-charged vortex solitons in harmonic potential, *Chaos Solitons Fractals* 171 (2023) 113422.